ELSEVIER

Journal of Atmospheric and Solar-Terrestrial Physics 67 (2005) 1566–1572

Journal of ATMOSPHERIC AND SOLAR-TERRESTRIAL PHYSICS

www.elsevier.com/locate/jastp

Predicted and measured slant ionospheric electron content

Miguel. A. Cabrera[a,c,*], R.G. Ezquer[a,b,c], S.M. Radicella[d]

[a]*Laboratorio de Ionósfera, Departamento de Física, Universidad Nacional de Tucumán, Argentina*
[b]*CONICET, Argentina*
[c]*Facultad Reg. Tucumán, Universidad Tecnológica Nacional, Argentina*
[d]*ARPL, Abdus Salam International Centre for Theoretical Physics, Italy*

Received 2 December 2004; received in revised form 14 June 2005; accepted 30 August 2005

Abstract

The total electron content (TEC) is used to indicate the ionisation of the ionosphere. TEC is a quantity with concern for telecommunications, detection systems, track, position, flight control and other systems that use transionospheric signals, because the ionospheric layer affects the mentioned signals.

In this work, the slant ionospheric electron content (SIEC) was modelled. The proposed method uses 'auxiliary' station that is determined over the slant link on terrestrial surface projection. This allows to obtain TEC between two points. Two models were considered, viz.: (i) the international reference ionosphere (IRI) and (ii) Chapman layer with scale height equal to atomic oxygen scale height (CHO).

The validity of the TEC calculated by both ionospheric models was checked with SIEC measurements obtained with geosynchronous satellites signals, for Boulder–ATS/6 and Palehua–ATS/6 links considering solstices and equinox, in low, moderate and high solar activity periods.

In general, in both links, the deviations between predictions and measurements were lower than 30% for about 10–14 h per day. In general, best model predictions are obtained during daylight hours.

The results suggest that additional studies for other links and solar activity are required.

Keywords: Electron content; Ionosphere; Transionospheric; Satellite; Models

1. Introduction

It is well known that the ionosphere produces several effects on transionospheric radio waves (Hargreaves, 1992). These effects are proportional to the number of free electrons encountered by the wave on its passage through the ionosphere (total electron content, TEC, Rishbeth and Garriot, 1969).

For aircraft navigation systems or satellite orbit determination, the satellite position and velocity are determined with the aid of radio signals transmitted between the satellite and the ground station (Harris et al., 2001). The ionospheric correction that has to be applied to determine the position accurately is proportional to the TEC along the radar–satellite path (Hartmann and Leitinger, 1984, among others). So, for ionospheric corrections, TEC

*Corresponding author. Laboratorio de Ionósfera, Departamento de Física, Universidad Nacional de Tucumán, Argentina. Tel./fax: +54 381 4363004.

E-mail address: mcabrera@herrera.unt.edu.ar (M.A. Cabrera).

1364-6826/$ - see front matter
doi:10.1016/j.jastp.2005.08.021

measurements are required, or TEC predictions from ionospheric models can be a useful tool.

Different ionospheric models have been developed to predict the electron density (N) distribution in height, which is called N profile (Anderson et al., 1985; among others), including the international reference ionosphere (IRI) model (Bilitza, 1990, 2001). With this N profile the vertical TEC can be obtained. Nevertheless, most of the signal paths are slant paths.

In general, to model the ionosphere, the so-called thin layer approximation is assumed the slant total electron content (STEC) is related with the vertical total electron content (VTEC) through the piercing point with the obliquity factor (Lin, 2001; Brunini et al, 2004, among others).

Taking into account that, in general, the ionospheric models give the vertical ionospheric electron content, the purpose of the paper is to study the performance of two models to calculate the slant ionospheric electron content (SIEC) between two points. A computation method and ionospheric model are used. We consider two widely used ionospheric models. One of them is the IRI, Rawer and Bilitza, 1990; Bilitza, 1990), an empirical model which is being improved and updated by contributions of the international scientific community. The other one is based on a theoretical frame, like the Chapman layer (Chapman, 1931), with scale height equal to atomic oxygen scale height, hereafter referred to as CHO.

2. Method

In general, the ionospheric models calculate the electron content only along the vertical. To obtain the slant electron content it is necessary to do the integration of the N profile along the ray path.

For this, we need to obtain the N profile along the oblique path. First, the length of the slant path (s–s') is divided in segments (j–$j+1$) of 20 km length. To obtain the N value at a point j of the slant path, it is needed to know the N value, given by the IRI and Chapman models, at the corresponding height of this point. To this end the models needs the geodetic coordinates of the point i obtained from the vertical projection of j point over the Earth surface. The i point is called 'auxiliary station'; see Fig. 1. Finally, the SIEC up to 2000 km is computed by numerical integration using the N profile obtained every 20 km along the signal path. For the calculus we assumed the Krasovsky geoid (Zakatov, 1981) and used the Simpson integration method (Sadosky, 1971).

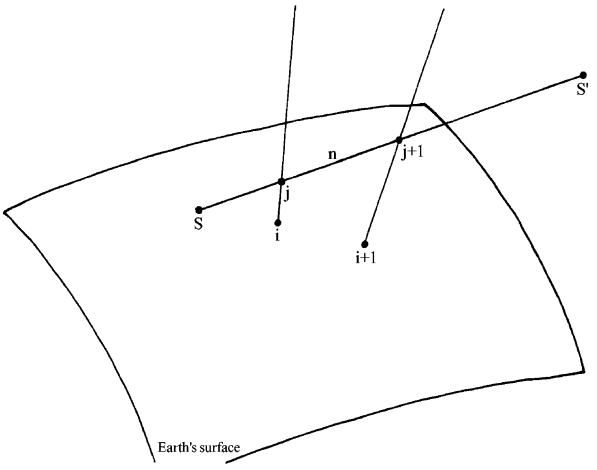

Fig. 1. s–s' is the slant path, j–$j+1$ determines the "n" segment and "i" is the Earth surface projection point called "auxiliary station".

3. Models and discussion

3.1. IRI

One of the most widely used empirical models is the IRI. It describes N in the altitude range from 50 to 2000 km for quiet magnetic conditions in the non-auroral ionosphere. IRI is the international standard for the specification of ionospheric densities and temperatures. It was developed and is being improved and updated by the joint working group of the International Radio Science (URSI) and the Committee on Space Research (COSPAR) (Bilitza, 2001). At the 1999 URSI General Assembly in Toronto, Canada, the URSI Commission G resolved that IRI be internationally recognised as the standard for the ionosphere.

In previous works (Cabrera et al., 2002; Ezquer et al., 2001) the slant electron content measurements obtained with the Faraday rotation technique at Palehua (21.4°N, 201.9°E) (Roelofs, 1980) and Boulder (40.1°N, 254.7°E) (Fritz, 1976) were used to compare with model predictions. Cabrera et al. (2002) calculated the slant electron content for the ATS/6–Palehua link. For the considered ray path the satellite was placed at (0°N, 200°E). The CCIR (CCIR, 1982) option was used to obtain the peak characteristics (NmF2, hmF2); equinoxes and

solstices were considered for middle solar activity period. Although overestimation was observed for night hours, the results showed good STEC predictions for several hours at the period of maximum ionisation. For the ATS/6–Boulder link, Ezquer et al. (2001) calculated the slant electron content for low solar activity year (July 1974–May 1975). The CCIR option was used to obtain the peak characteristics. The comparison with experimental data showed cases with very good agreement between predictions and measurements (July and August for hours of minimum STEC). But, in general, the model underestimated the STEC.

3.2. Chapman layer

The Chapman layer offers a simple way to explain the vertical structure of plasma in the upper atmosphere. (Chapman, 1931; Huang and Reinisch, 2001; Reinisch et al., 2004, among others). It should be noted that in spite of the physical process occurring in the ionosphere being different from those assumed by Chapman in the original deriving, many authors have shown that the shape of the vertical electron density profile (N) tends to a Chapman profile as time elapses (Yonezawa, 1955; Wright, 1960; Yonezawa and Takahashi, 1960).

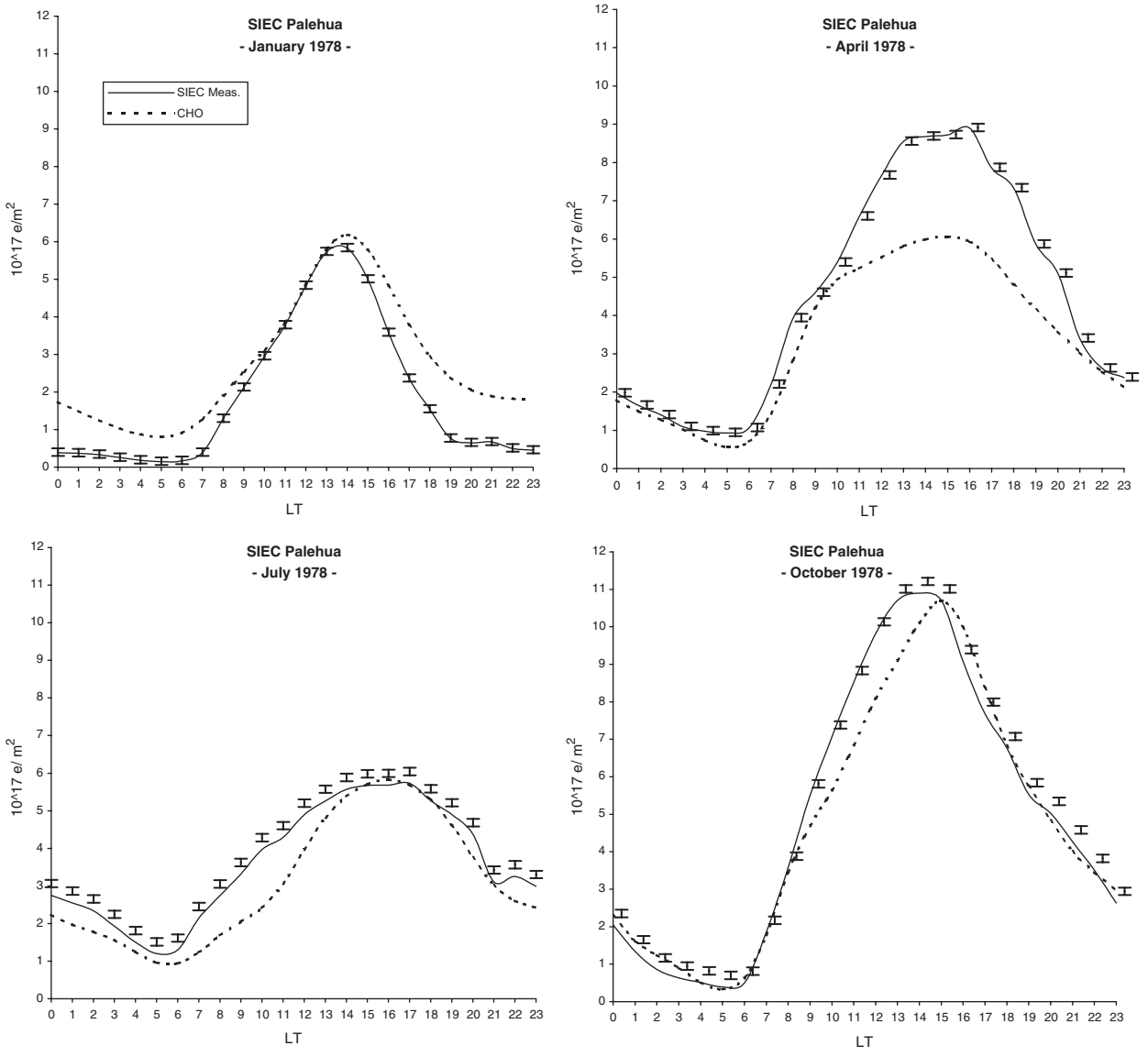

Fig. 2. SIEC measurements and model predictions for Palehua–ATS-6 satellite radio signal path. The bars indicate the absolute deviation.

Wright (1960) has shown that it is possible to apply the following Chapman expression to the F region:

$$N(z) = N_m \exp\{0.5[1 - z - \exp(-z)]\}, \quad (1)$$

where z is the $(h-h_m)/H$ is the normalised height measured from h_m in units of the scale height H. He proposed to take H as the scale height of atomic oxygen. In this paper we assume the Chapman expression given by Eq. (1) with H equal to atomic oxygen scale height. N_m and h_m correspond to peak characteristics and are obtained from CCIR global maps. H was calculated using $H = kT/mg$, where k, T, m and g are Boltzmann's constant, neutral temperature, atomic oxygen mass and the acceleration due to gravity, respectively. The value of T is obtained from the MSIS-86 model (Hedin, 1987).

The purpose of the paper is to determine monthly mean values of SIEC. The model predictions are compared with measurements obtained using ATS-6 geosynchronous satellite signals received at Palehua (Roelofs, 1980) and Boulder (Fritz, 1976), stations placed in the low and middle latitudes. The data obtained with geosynchronous satellite allow high temporal resolution for a fixed link. The Faraday technique gives the electron content without the plasmaspheric contribution.

Fig. 2 shows the calculated SIEC for ATS/6–Palehua (21.4°N, 201.9°E) link. For the considered ray path the satellite was placed at (0°N, 200°E). Equinoxes and solstices are considered for the high solar activity period. It can be seen that, in general, there is a good agreement between CHO model predictions and measurements for October

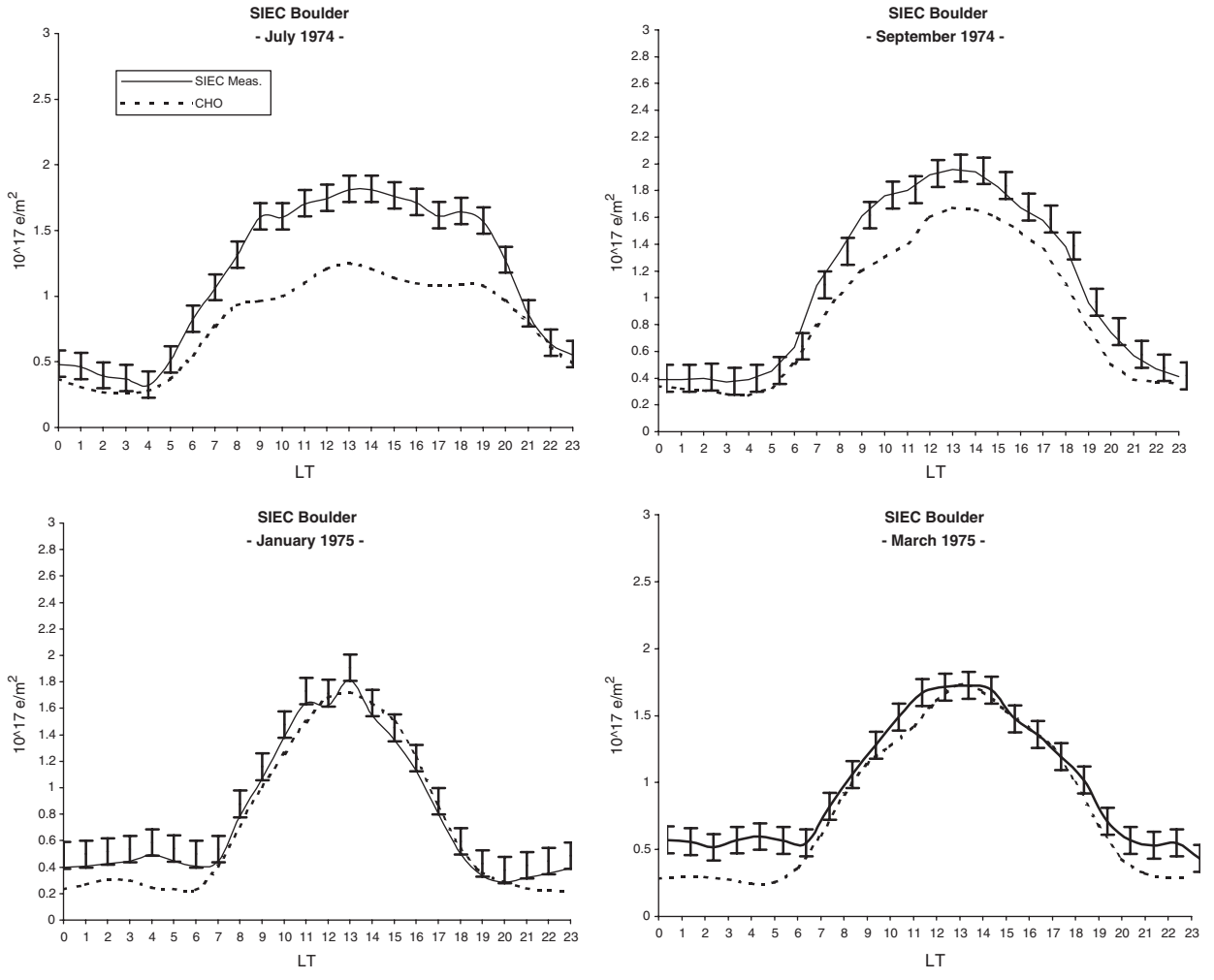

Fig. 3. SIEC measurements and model predictions for Boulder–ATS-6 satellite radio signal path. The bars indicate the absolute deviation.

and July. For October 1978 it is possible to see a good absolute agreement for [3–8] LT and [18–22] LT periods; for [23–03] LT and [8–18] LT periods, a good relative agreement is observed. For July 1978 it is possible to see a good absolute agreement for [04–05] LT and [14–21] LT periods, and for [05–14] LT and [21–04] LT periods, a good relative agreement is observed. The worst predictions are observed for January solstice; in general, the model overestimates the measurements and shows good agreement around noon for the [10–13] LT period. For April 1978 it is possible to see good absolute agreement for the [22–04] LT period, and for [04–22] LT period, an underestimation is observed.

Fig. 3 shows the results for Boulder (40.1°N, 254.7°E)–ATS-6 satellite radio signal path, for low solar activity year. Equinoxes and solstices are considered.

It can be seen that the model underestimates STEC values in some cases. The worst predictions correspond to July, with good absolute agreement; only for the [21–04] LT period an underestimation is observed for the [04–21] LT period. The underestimation observed for September, in general, is about 20%, and for the [07–18] LT period, a good relative agreement is observed. For the [18–07] LT period it is possible to see a good absolute agreement. The best absolutes agreements are obtained for January and March.

In order to sum up the results obtained with IRI model in previous works (Cabrera et al., 2002; Ezquer et al., 2001), Table 1 shows the deviations (D) between modelled values and measurements. The coefficient D was calculated using the following expression:

$$D = \left| \frac{(\text{predicted SIEC} - \text{measured SIEC})}{\text{measured SIEC}} \right|.$$

The white, light grey and dark grey boxes correspond to the cases where $D \leqslant 30\%$, $30 < D \leqslant 50\%$ and $D > 50\%$, respectively. The best agreement is obtained for Palehua July high solar activity, and high values are observed for nighttime hours in some cases. For Boulder, January and March low solar activity, the coefficient D reaches high values for daylight hours. Nevertheless, it can be seen that, in general, the deviation is lower than 30% since 08–17 LT.

The results obtained with CHO model are summarised in Table 2. It can be seen that the number of green boxes is greater than those

Table 1

IRI	BOULDER				PALEHUA			
Date	Jan-75	mar-75	jul-74	sep-74	Jan-78	Apr-78	jul-78	oct-78
R_{12}	24	21	34	32	61	77	97	111
0 LT	26.0	24.4	53.3	77.9	261.0	86.3	29.5	74.0
1	38.0	32.4	34.6	70.5	236.9	92.1	29.0	109.7
2	44.7	48.5	43.1	59.8	254.4	91.4	29.9	173.0
3	36.3	23.8	45.4	58.6	312.7	102.8	43.0	199.2
4	0.4	3.0	77.8	42.1	314.1	75.9	55.3	149.0
5	11.2	10.7	41.0	45.6	241.8	52.0	60.8	138.6
6	16.3	57.3	23.2	52.9	253.0	53.8	46.2	193.4
7	74.1	52.1	25.5	26.6	230.7	12.3	8.9	58.1
8	54.1	62.2	18.3	25.4	15.5	9.2	5.8	30.3
9	46.3	54.0	1.9	14.3	71.7	3.0	1.2	5.8
10	31.4	41.6	1.9	11.4	44.7	5.2	2.0	6.6
11	25.1	36.1	0.6	18.3	21.7	9.6	6.8	11.0
12	36.9	45.5	4.6	20.3	2.5	8.2	9.8	13.2
13	23.0	51.2	2.2	21.9	7.3	8.8	13.9	14.9
14	37.0	49.5	1.1	21.1	7.4	6.2	15.4	10.3
15	44.1	58.1	2.8	21.9	5.2	7.1	17.8	4.7
16	46.9	58.8	3.5	26.3	36.3	12.4	17.8	2.1
17	5.2	65.3	1.9	22.8	78.4	5.7	15.2	12.5
18	68.5	61.8	2.4	18.1	116.9	6.7	19.0	7.7
19	87.2	76.1	6.4	27.1	242.9	3.4	15.9	17.5
20	88.4	60.8	20.5	18.6	246.2	4.1	13.3	16.1
21	51.4	38.9	51.2	26.7	214.4	37.1	38.3	22.2
22	29.5	15.1	68.8	51.3	287.6	63.4	20.9	35.3
23	17.0	71.6	50.7	75.6	266.7	68.9	26.1	62.7

Table 2

CHO	BOULDER				PALEHUA			
Date	Jan-75	mar-74	jul-74	sep-74	Jan-78	Apr-78	jul-78	oct-78
R_{12}	24	21	34	32	61	77	97	111
0 LT	41.7	41.3	22.9	12.8	349.4	9.1	18.9	12.3
1	33.8	36.9	32.6	17.9	304.3	9.7	22.7	20.9
2	29.5	30.1	30.8	22.5	275.4	8.6	23.9	44.7
3	32.4	42.1	29.7	24.3	308.7	5.5	19.2	42.5
4	50.7	51.5	12.5	30.8	375.5	24.4	16.7	0.0
5	47.2	46.1	27.5	26.7	450.7	40.3	19.7	15.4
6	43.7	19.9	32.9	19.0	441.1	33.6	28.0	25.5
7	8.1	17.0	27.4	27.5	230.7	34.5	42.5	4.8
8	9.3	5.9	29.0	23.1	47.3	28.0	38.7	3.6
9	5.3	4.0	40.0	25.5	19.8	8.7	38.1	14.7
10	9.0	9.2	37.5	26.1	5.8	8.5	39.3	20.2
11	8.5	10.1	35.3	21.7	1.9	20.6	28.7	19.7
12	3.6	0.7	30.5	16.7	0.4	27.9	18.8	17.6
13	5.1	5.9	30.9	14.8	1.2	32.0	8.4	15.0
14	6.0	5.1	33.1	14.4	6.0	31.0	3.4	7.3
15	10.3	11.2	35.2	12.6	15.6	30.5	0.5	0.0
16	8.8	11.4	35.7	10.2	34.9	33.4	2.5	10.1
17	6.6	14.4	32.9	13.9	60.2	30.4	0.7	9.1
18	7.1	7.4	33.5	20.3	90.9	34.4	0.4	1.2
19	8.1	9.0	31.2	19.8	212.8	29.2	5.9	4.2
20	1.8	9.0	24.4	31.1	218.4	29.6	14.0	4.0
21	25.1	27.0	8.1	31.6	182.9	10.6	2.9	6.1
22	37.5	36.7	3.1	21.3	265.5	3.1	19.7	1.4
23	45.3	16.7	10.9	12.2	302.2	10.9	19.1	12.5

observed in Table 1. Similar results are obtained for Palehua January, with both models. Few cases show deviations greater than 50% and they correspond to nighttime hours.

For the considered cases, the comparison of the tables suggests that CHO model has a better performance than IRI to predict the SIEC.

4. Conclusions

It was shown that is possible to calculate slant ionospheric electron content using vertical electron density profiles. Two models were considered, the international reference ionosphere (IRI) and Chapman layer with scale height equal to atomic oxygen scale height (CHO).

The models predictions were checked with SIEC measurements obtained with geosynchronous satellites signals, for Boulder–ATS-6 and Palehua–ATS-6 links, considering solstices and equinox, in low, moderate and high solar activity years. Monthly values were considered.

For the considered cases, the results suggest that CHO model show a better performance than IRI to predict the SIEC. In general, in both links, the deviations between predictions and measurements were lower than 30% for about 10–14 h per day. In general, best model predictions are obtained during daylight hours.

Taking into account that the SIEC values were calculated using the CCIR option in both models, the better performance of CHO suggests that the shape of the N profile of this model is more realistic than that assumed by IRI.

The observed disagreements between predictions and measurements could arise because peak characteristics or the shape of N profile, or both are not well predicted.

Additional works for other links and conditions are required in order to study the performance of the models to predict SIEC.

References

Anderson, D.N., Mendillo, M., Herniter, B., 1985. A semi-empirical, low-latitude ionospheric model, Air Force Geophysics Laboratory Report AFGL-TR-85-0254, Hanscom AFB, MA.

Bilitza, D., 1990. International reference ionosphere. NSSDC/WDC-A-R&S 90-22, MD, EEUU.

Bilitza, D., 2001. International reference ionosphere. Radio Science 36, 261–275.

Brunini, C., Meza, A., Azpilicuata, F., Van Zele, M.A., Gende, M., Díaz, A., 2004. A new ionosphere monitoring technology based on GPS. Astrophysics and Space Science 290, 415–429.

Cabrera, M.A, Ezquer, R.G., Mosert, M., Jadur, C.A., 2002. Comparison of experimental slant electrón content and IRI model. In: Proceedings of the IRI Task Force Activity, IC/IR 2002/23, August 2001, Trieste, Italy. p. 162. ISBN 92 95003 14-4.

CCIR, 1982. Comité Consultatif International des radiocommunications. International Telecomunication Union, Place des Nations, Switzerland, 1982.

Chapman, S., 1931. The absorption and dissociative or ionizing effect of monochromatic radiation in the atmosphere on a rotating Earth. Proceedings of the Physical Society of London 43, 26.

Ezquer, R.G., Jadur, C.A., Radicella, S.M., Kiorcheff, E., Oviedo, R.del.V., Manzano, J.R., Scidá, L., 2001. IRI Slant electron content predictions. Advances in Space Research 27 (1), 65.

Fritz, R.B., 1976. ATS-6 radio beacon electron content measurements at Boulder , July 1974–May 1975. Report UAG-58, WDC, CO, 1976.

Hargreaves, J.K., 1992. The Solar-Terrestrial Environment, Cambridge Atmospheric and Space Science Series. Cambridge University Press, Cambridge.

Harris, I.L., Mannucci, A.J., Iijima, B.A., Lindqwister, U.J., Muna, D., Pi, X., Wilson, B.D., 2001. Ionospheric specification algorithms for precise GPS-based aircraft navigation. Radio Science 36 (2), 287–298.

Hartmann, G.K., Leitinger, R., 1984. Range error due to ionospheric and tropospheric effects for signals frequencies above 100 MHz. Bulletin Geodesique 58, 109–136.

Hedin, A.E., 1987. MSIS-86 thermosphere model. Journal of Geophysical Research 92, 4649.

Huang, X., Reinisch, B., 2001. Vertical electron content from ionograms in real time. Radio Science 36 (2), 335–342.

Lin, Lao-Sheng, 2001. Remote sensing of ionosphere using GPS measurements. In: Proceedings Asian Association on Remote Sensing, Singapore. vol. 1, pp. 69–74.

Rawer, K., Bilitza, D., 1990. International reference ionosphere—plasma densities: status 1988. Advances in Space Research 10 (8), 5–14.

Reinisch, B.W., Huang, X.-Q., Belehaki, A., Shi, J.-K., Zhang, M.-L., Ilma, R., 2004. Modeling the IRI topside profile using scale heights from ground-based ionosonde measurements. Advances in Space Research 34, 2026–2031.

Rishbeth, H., Garriot, O.K., 1969. An Introduction to Ionospheric Physics. Academic Press, New York.

Roelofs, T.H., 1980. Plasmapheric, Faraday and total electron contents, 1977 and 1978. Report AFGL-TR-81-0143, University of Hawaii, Honolulu, Hawaii. (Final report.)

Sadosky, M., 1971. Cálculo Numérico y Gráfico. (Ed.) Librería del Colegio, Buenos Aires.

Wright, J.W., 1960. A model of the F region above $h_{\max}F2$. Journal of Geophysical Research 65 (1).

Yonezawa, T., 1955. On influence of the electron–ion diffusion on the electron density and height of the nocturnal F2 layer. Journal of the Radio Research Laboratory, Japan 2.

Yonezawa, T., Takahashi, H., 1960. On the electron and ion density distributions from the lower uppermost part of the F region. Journal of the Radio Research Laboratories 7 (32), 1960.

Zakatov, P.S., 1981. Curso Superior de Geodesia. (Ed.), MIR, Moscow.